

Patient-derived Tumor Spheroid Cultures as a Promising Tool to Assist Personalized Therapeutic Decisions

Sarah Hofmann

Institute for Personalized and Medical Research

Raichel Cohen-Harazi (✉ raichelha@ariel.ac.il)

Institute for Translational and Personalized Medicine

Yael Maizels

Institute for Personalized and Translational Medicine

Igor Koman

Institute for Personalized and Translational Medicine

Research

Keywords: 3D models, personalized medicine, patient-derived spheroids, breast cancer

DOI: <https://doi.org/10.21203/rs.3.rs-35980/v1>

License:  This work is licensed under a Creative Commons Attribution 4.0 International License.

[Read Full License](#)

Abstract

Background

Breast cancer is the most common cause of cancer-related death in women. Treatment of breast cancer has many limitations including a lack of accurate biomarkers to predict success of chemotherapy, intrinsic resistance of a significant group of patients to the gold standard of therapy and the limited applicability of targeted therapy. Therefore, new tools are needed to provide doctors with guidance in choosing the most effective treatment plan for a particular patient and thus to increase the survival rate for breast cancer patients.

Methods

Here, we present a successful method to grow in vitro spheroids from primary breast cancer tissue. Samples were received in accordance with relevant ethical guidelines and regulations. After tissue dissociation, in vitro spheroids were generated in a scaffold-free 96-well plate format. Spheroid composition was investigated by immunohistochemistry (IHC) of epithelial (Pan Cytokeratin (panCK)), stromal (Vimentin) and breast cancer-specific markers (ER, PR, Her2, GATA, Mammaglobin). Growth and cell viability of the spheroids was assessed upon treatment with multiple anti-cancer compounds. Student's t-test and two-way ANOVA test were used for statistical analysis.

Results

We were able to successfully grow spheroids from 27 out of 31 samples from surgical resections of breast cancer tissue from previously untreated patients. Recapitulation of the histopathology of the tissue of origin was confirmed. Furthermore, a drug panel of standard first line chemotherapy drugs used to treat breast cancer was applied to assess the viability of the patient-derived spheroids and revealed variation in the response of the spheroids to different drug treatments.

Conclusions

We investigated the feasibility and the utility of an in vitro, patient-derived spheroid model for breast cancer therapy, and we conclude that spheroids serve as a highly efficient platform to explore cancer therapeutics and personalized treatment efficacy.

These results have significant implications for the application of this model in clinical personalized medicine.

Introduction

Breast cancer is the most common cause of cancer related deaths for women worldwide. In Europe alone, approximately 630,000 women died from breast cancer in 2018. According to current European and American guidelines for treatment, breast cancers are categorized into molecular subtypes based on the

expression of hormone receptors PR and ER as well as Her2 and Ki67. The subtypes include Luminal A, Luminal B, Her2+/non-luminal, and basal-like/triple negative, and each subtype has its own course of treatment. For the luminal subtypes, treatment includes endocrine therapy and for the Her2+/non-luminal subtype treatment includes the anti-Her2 drug trastuzumab (Cardoso et al., 2019; Duffy et al., 2017; Howlader et al., 2018; Telli et al., 2019). In addition, for the luminal A subtype there are a variety of new drugs that target specific pathways such as Everolimus for mTOR, Abemaciclib, Palbociclib, Ribociclib for CDK 4/6, and Olaparib for those with BRCA1/2 mutations (Telli et al., 2019). While a variety of options of targeted drugs is promising, they are only relevant for those with the relevant molecular background. This means these solutions are relevant for only a small group, for example only 2–3% of breast cancer patients have BRCA1/2 mutations (Griguolo et al., 2018). In addition, it has been shown that intrinsically tamoxifen resistant cancers often have a large number of gene alterations, making the choice of an alternative therapy anything but straightforward (Hultsch et al., 2018; Poudel et al., 2019). Yet, for the basal-like/triple negative subtype where neither endocrine therapy or anti-Her2 therapy is appropriate, the first line of therapy is classic chemotherapy (Denkert et al., 2017; Yuan et al., 2019) and there is only one approved immunotherapy drug, Atezolizumab (Heimes and Schmidt, 2019). In recent years, it has been demonstrated that targeted therapies that were approved for one indication may be effective in treating others, this is known as drug repurposing. For example, the drug that targets the mTOR pathway, Everolimus that was originally developed as an immunosuppressant drug for transplant patients, is now approved for use in luminal A breast cancer (Neumayer et al., 1999; O’Shaughnessy et al., 2018). New targeted or immunotherapy drugs, that can treat the basal-like/triple negative may already exist.

In addition to endocrine therapy and anti-Her2 drugs, the majority of patients are treated according to a conventional chemotherapy protocol which includes anthracyclines and/or taxanes, with few known biomarkers for predicting response to a given treatment (Cardoso et al., 2019; Denkert et al., 2017; Duffy et al., 2017; Gu et al., 2016). Drug choice is also complicated for targeted therapy, as sometimes there are several drugs that target the same pathway and there are no clear biomarkers to help with the choice of which targeted drug to use. An unguided choice for first line therapy can lead to a delay in effective treatment, and thus risk progression of the disease. Furthermore, each course of treatment is accompanied by suffering due to adverse side effects of chemotherapy (Fotheringham et al., 2019; Jensen, 2006). Even when actionable biomarkers do exist, their diagnostic value is not individual, and some patients may not respond to the predicted therapy. Later, some patients who initially respond to the treatment may develop recurrence and progression of the disease (Bastien et al., 2015; Gu et al., 2016; de Melo Gagliato et al., 2016). New tools to predict drug efficacy for individual patients would extend survival and prevent treatment with ineffective drugs. In summary, new tools for treatment selection are needed to give doctors guidance where no biomarkers currently exist, to predict when patients may not respond to targeted options, to explore opportunities for drug repurposing and to assay drug efficacy where drug toxicity and the risk of side effects is high. Expanding the field in these ways will lead to more effective treatment plans, better quality of life for patients and fewer breast cancer deaths.

One approach to developing new tools to guide individualized treatment selection utilizes chemotherapy sensitivity and resistance assays (CSRAs) which use viable tissue from a tumor to provide predictive

information about response to treatment (Burstein et al., 2011; Morgan et al., 2016). These techniques have the benefit of being inexpensive, quick and compatible with high-throughput screening to help guide treatment decision making (Morgan et al., 2016). Initially, assays were developed using cells from tumors in two dimensional (2D) tissue culture (Joo et al., 2009; Ochs et al., 2005). Yet, 2D culture of tumor cells does not accurately mimic the complex relationship between the cells, and the access to oxygen, nutrients and signaling molecules. Furthermore, in the 2D culturing process, there is selection of specific cell populations and the cells undergo significant changes in gene expression (Hickman et al., 2014; I, et al., 2010; Jo et al., 2018; Morgan et al., 2016; Richard et al., 2015; Weiswald et al., 2015). To address these limitations, a number of three dimensional (3D) models have been developed including tumor cells seeded in a matrix of extracellular proteins, multicellular tumor spheroids, organoids, tissue slices, and bioreactors and microfluidic models (Brancato et al., 2020; Grinshpun et al., 2018; Jo et al., 2018; Majumder et al., 2015; Morgan et al., 2016; Mulholland et al., 2018; Oritura et al., 2018; Tanigawa et al., 2016; Weiswald et al., 2015).

Our work focuses on one type of 3D model, namely spheroids, which are scaffold-free multicellular spheres containing cancer cells. These spheroids take into account cell-cell interactions and can facilitate the production of the endogenous extracellular matrix to provide local tumor microenvironment-like conditions. Additional environmental considerations, including the access to nutrients, oxygen, growth factors, metabolites and paracrine factors, are also recapitulated (Brancato et al., 2020; Weiswald et al., 2015). The microtissue culture system from InSphero AG, Switzerland (3D InSight™ system) has been used to create multicellular tumor spheroids from a single cell suspension using a range of tissue culture lines (Anastasov et al., 2015; Falkenberg et al., 2015, 2016; Herter et al., 2017; Rimann et al., 2014; Thoma et al., 2013) and patient derived samples from osteoblastic, chondroblastic and renal cell carcinoma (Amann et al., 2014; Bolck et al., 2019). A similar technique was used by Shuford, et al. who demonstrated that spheroid cultures could be generated from patient-derived ovarian tissue samples with a 90% success rate, with an overall accurate prediction of response to first-line accuracy in 89% of samples. This clearly demonstrates the potential of this method to facilitate treatment choice, as well as to explore non-standard therapies, both of which would prevent a delay in effective treatment, eliminate unnecessary suffering, and ultimately improve prognosis. Still, in the study cited above, 11% of results were falsely negative, with the spheroids indicating no response and the actual patient showing a response. Clearly, this method requires further improvement (Shuford et al., 2019). There are currently no clinically recommended CSRAs by the American Society of Clinical Oncology but their potential, following further development, is acknowledged (Burstein et al., 2011). As more studies show the utility and efficacy of such models, we are confident that they will be integrated into the medical decision-making pipeline.

Here, we present a successful method to grow in vitro spheroids from patient-derived tumor tissue. Our model is demonstrated on breast cancer, and will be further expanded to include additional histotypes in future pro- and retrospective studies.

Results

Generation of spheroids from surgical samples of human breast cancer tissue

In order to establish a working protocol to grow in vitro spheroids from human patient material, tissue samples were received post-surgery from previously untreated human breast cancer patients (Fig. 1). After dissociation of the tissue into single cell suspension, spheroids were generated using a scaffold-free approach in the 96-well plate format from InSphero 3D InSight™ (GravityTRAP™ and GravityPLUS™) Hanging Drop System or the Corning® Ultra-Low Attachment (ULA) spheroid microplates. We observed that the reconstitution of the tumor microenvironment with stromal cells using normal human fibroblasts, was fundamental to ensure the generation of multicellular aggregates in stable tumor spheroids. The best results were achieved with a tumor cell-to-fibroblast ratio of 1:3, but a 1:1 ratio also produced fairly smooth spheroids (Fig. 2). The fibroblasts are recognized by the epithelial cells, and serve as a scaffold to facilitate the self-assembly of the tumor cells. On average, complete cell agglomeration into compact spheroid was seen after 2–4 days under optimal culture conditions. Once formed, spheroids could be fixed and stained for IHC or immunofluorescence (IF), monitored for growth by light microscopy and/or viability assay or treated with a panel of chemotherapy drugs (see Fig. 1).

Spheroid growth success rate is consistent across breast cancer tissues with distinct molecular signatures

We received surgical samples from a cohort of 31 breast cancer patients and were able to successfully grow spheroids from 27 out of the 31 samples, with an overall success rate of 88%. We had access to pathological and clinical data for most of the original tissue material. Table 1 shows a summary of the samples used in the study, with the available information regarding tumor stage and genetic background, as well as the success rate of establishing spheroids from the given tissues. Spheroid growth success rate was independent of these tumor features based on the intrinsic data set. It is important to note that all samples from the triple-negative subtype were successfully grown using this procedure. This is encouraging since there is a lack of targeted drugs for this particular subtype (Cardoso et al., 2019; Heimes and Schmidt, 2019; Jamdade et al., 2015; Telli et al., 2019). Thus, our established working protocol can generate in vitro spheroids from breast cancer tissues of different stages and genetic backgrounds.

Table 1: 3D spheroids were grown from breast cancer samples of varying stages and genetic backgrounds with an 87% success rate. Overall, 31 human tissue samples from breast cancer patients of different tumor stage, genetic background and Ki67 level were received and seeded into spheroids. The success rate for generating spheroids was 87%.

Tumor stage	I-II	II	II-III	III	N/A	total
Total number of samples	4	9	4	5	9	31
Successful samples (%)	4 (100%)	7 (78%)	4 (100%)	4 (80%)	8 (88%)	27 (87%)

Genetic background	Triple negative	Luminal A	Luminal B (i)	Luminal B (ii)	N/A	total
Total number of samples	4	11	9	5	2	31
Successful samples (%)	4 (100%)	10 (91%)	7 (78%)	4 (80%)	2 (100%)	27 (87%)

Ki67	0-10%	11-20%	21-40%	N/A	total
Total number of samples	17	6	3	5	31
Successful samples (%)	15 (88%)	6 (100%)	3 (100%)	3 (60%)	27 (87%)

IHC confirms histopathological composition of spheroids

The promising results achieved in generating in vitro spheroids from breast tumor of human origin, prompted us to determine the cellular composition of these spheroids and their resemblance to the original tissue. For this, spheroids cultured in the InSphero 3D InSight™ or Corning® ULA microplates, were fixed with paraformaldehyde and characterized by IHC. We found that spheroids generated from breast tissue contained both epithelial cells (as shown by panCK staining) and stromal cells (indicated by Vimentin staining) (see Fig. 3). The epithelial cells in the spheroid are of tumor tissue origin, demonstrating that our technique supports the growth of original tumor tissue in the spheroid model. As expected, spheroids that were generated from human dermal fibroblasts (HDFs) alone, did not stain positive for any breast cancer markers and only stained positive for Vimentin (see Fig. 3). Once we showed that tumor cells integrate into our spheroids, we investigated whether they maintain the molecular characteristics of the original tumor. Figure 3 shows a representative example of an original tumor, identified as ER+, PR- and Her2- and classified as Luminal B (i) (Cardoso et al., 2019). IHC staining of the spheroids for these markers revealed that, like the original tissue, the spheroids were PR and Her2 negative. There was a small population of ER+ cells in the original tumor and in the spheroids. We then went on to stain for two more markers for breast cancer, GATA-3 and Mammaglobin, that are commonly expressed in luminal B breast cancer (over 90% and 50% respectively) (Ni et al., 2018). GATA-3 was expressed in individual cells in the original tumor and the spheroid while mammaglobin was expressed in both the spheroid and the original tissue in clusters of cells.

Spheroids respond to standard chemotherapy drugs.

After successfully growing breast cancer spheroids from a variety of different breast cancer patients and confirming that the spheroids reflect the molecular characteristics of the original tissue, we investigated whether this model could serve as a platform to test drug sensitivity. Chemotherapy is commonly used in all subtypes of breast cancer except luminal A, depending on the risk of recurrence. The most commonly used chemotherapy drugs are anthracyclines (Doxorubicin (Doxo) and Epirubicin (Epi)) and/or taxanes

(Paclitaxel (Pac) and Docetaxel) (Cardoso et al., 2019; Jensen, 2006). We generated spheroids from breast cancer tissue using the InSphero 3D InSight™ 96-well plate system and assayed for spheroid growth and cell viability (Fig. 4A). After three days in culture, we treated the spheroids with Doxo (Fig. 4B), a standard drug used to treat early breast cancer which has cardiotoxic effects (Cardoso et al., 2019; Jensen, 2006). Spheroid growth was monitored over 6 days of treatment and a clear shrinking of the tumor was observed (Fig. 4C). Following 7 days of incubation with Doxo, we measured the cellular viability of treated spheroids using a luminescence-based ATP assay. We found a significant decrease in intracellular ATP levels in Doxo-treated spheroids, which correlated with the reduction in tumor volume (Fig. 4D).

Next, to test the feasibility of the 3D spheroid model as a drug screening model, breast cancer patient-derived spheroids were used for the screening of FDA-approved drugs. For selection of the treatments to be included in the drug panel, we referred to the American Cancer Society (www.cancer.org/cancer/breast-cancer/treatment/chemotherapy-for-breast-cancer.html) and the cancer.net (www.cancer.net/cancer-types/breast-cancer/types-treatment) websites and generated a short-list of approved chemotherapeutic drugs commonly used to treat breast cancer. The list included Pac, Epi, 5-Fluorouracil (5-FU) and Metformin (Met). Pac and Epi are routinely administered as first-line chemotherapy drugs for early and late stage breast cancer and 5-FU is sometimes used in combination with cyclophosphamide and methotrexate (Cardoso et al., 2019; Coates et al., 2015; Huang and Campbell, 2012; Walsh and Goodman, 2002; Zoli et al., 2005). In contrast, Met has recently been reported to provide a promising adjuvant treatment for prostate and colorectal cancer and is currently being investigated as adjuvant therapy for breast cancer in an active phase III clinical trial (NCT01101438, Coyle et al., 2016). We used Met in our drug panel as an example of an experimental drug for breast cancer.

Spheroids were generated using the InSphero 3D InSight™ system and, following 4 days of incubation under optimal growth conditions, were treated with Pac, Epi, 5-FU and Met for a period of up to one week (Fig. 5A). The concentration of each drug was chosen from previous studies on 2D models and increased accordingly to the 3D setup (Buxant et al., 2017; Garbar et al., 2017; Zasadil et al., 2014; Zoli et al., 2005). Spheroid size was monitored by light microscopy, and the area was determined (Fig. 5B). The size of the spheroids decreased significantly upon treatment with 5-FU (Fig. 5C). Pac and Epi treatments led to a visible reduction in spheroid size (Fig. 5B), but statistical significance could only be seen when applying a 90% confidence interval (data not shown). Following treatment, ATP levels were measured using the luminescence-based ATP assay (Fig. 5D). As expected, ATP levels significantly decreased under treatment with the first-line chemotherapy drugs for breast cancer, Pac, 5-FU and Epi, while Met showed no reduction in ATP levels (Fig. 5D) or spheroid size (Fig. 5B and 5C). Thus, the patient-derived spheroids respond, with expected variability, to clinically relevant chemotherapy drugs. Our system, therefore, has the potential to be utilized as a tool for personalized prediction of the responsiveness of cancerous tissue to a selected chemotherapeutic option. Further optimization and validation of our protocol will be performed in future pro- and retrospective studies.

Discussion:

Improved method to generate spheroids from human breast cancer tissue

In this study we present an improved method for generating spheroids from cancerous human breast tissue. The generation of spheroids and other types of 3D models from cell lines has already been reported (Anastasov et al., 2015; Falkenberg et al., 2015, 2016; Herter et al., 2017; Ho et al., 2012; Lee et al., 2007; Rimann et al., 2014; Thoma et al., 2013). And several publications about patient-derived 3D models have also demonstrated their potential for application in personalized medicine (Amann et al., 2014; Bolck et al., 2019; Goldman et al., 2015; Grinshpun et al., 2018; Halfter et al., 2016; Joo et al., 2009; Majumder et al., 2015; Morgan et al., 2016; Orditura et al., 2018; Tanigawa et al., 2016). Here, we used material derived from a cohort of breast cancer patients to establish an effective protocol for the generation of spheroids utilizing a scaffold-free approach and tested their applicability in a variety of end-point assays.

Our success rate in growing spheroids from primary tissue was at 88%, which is significantly higher than previously reported for work on patient-derived 3D models (e.g. Miyoshi et al. reported a success rate of 73% in patient-derived colorectal spheroids (Miyoshi et al., 2018)). Spheroids which failed to grow (4 out of 31) were mostly due to contamination with bacteria or fungi (in 3 cases), or low quality of the original tissue piece which resulted in a low yield of viable epithelial cells after single cell extraction (in 1 case).

In addition to generating breast cancer spheroids, we were also able to grow spheroids from a wide variety of patient-derived tissues, including stomach, esophagus, skin and prostate (data not shown). We employed a generic growth media that was supplemented with necessary growth factors and additives, such as insulin, heparin or hydrocortisone, as well as beta-estradiol. We did, however, refrain from adding stem cell niche factors, in order to avoid selective growth of only one particular subpopulation (Yin et al., 2016). It is important to note that we observed the essential role of adding normal fibroblast cells for the spheroid formation process. Stromal cells are indispensable to the 3D architecture of the tissue. They contribute to the physical cell organization and to the biochemical signaling within the tumor microenvironment, and thus support key properties of solid tumors. Fostering cell-cell interactions between normal fibroblasts and cancer epithelial cells within the spheroids is therefore critically important for mimicking the tumor microenvironment in vitro (Herter et al., 2017; Kijima et al., 2019; Thoma et al., 2014; Weydert et al., 2020; Whelan et al., 2018). Since it is well known that the addition of exogenous normal fibroblasts may alter the spheroid composition, we carefully chose the supplements of the growth media. For example, FGF10 has been reported to selectively promote epithelial cancer cell growth, while cholera toxin reduces the expansion of fibroblasts (Hollenberg and Cuatrecasas, 1973; Memarzadeh et al., 2007; Mulholland et al., 2018). In addition, in most cases, the spheroids were cultured for a maximum of 2 weeks in medium with a low percentage of serum, thereby also limiting the expansion of the fibroblast population.

Validation of spheroid composition

In order to better understand the specific spheroid composition, we performed immunohistochemical analysis to identify and discriminate between the epithelial and stromal cells. It has previously been shown that in spheroids generated from co-cultures of cancer cell lines and fibroblast lines the epithelial cells are primarily localized to the periphery of the spheroid, whereas the fibroblast cells make up the core (Amann et al., 2014; Herter et al., 2017). Surprisingly, and in contrast to what we and others have seen in spheroids from co-cultured cell lines, we did not detect a clear and distinct localization of epithelial and stromal cells in the spheroids generated from patient-derived material (see Fig. 3 as a representative image of our consistent observation of this phenomenon).

In addition, we showed that the composition of the spheroids recapitulates the molecular features of the original tissue with regards to the classic breast cancer markers ER, PR and Her2. Since these markers are standard in the clinic to characterize the tumor it is important to note that their expression was maintained in the spheroid model. We further characterized the spheroids by looking at two additional common breast cancer markers, GATA-3 and mammaglobin, and saw that these markers were expressed both in the original tissue and in the tumor spheroids. These data provide an important piece in the validation of our method.

Responsiveness of spheroids to drug panel

To provide a preliminary proof-of-concept that spheroids could, indeed, be utilized as in vitro models for the prediction of drug response in personalized medicine, we applied a small panel of commonly used chemotherapy and adjuvant drugs, including Pac, Epi, 5-FU and Met onto spheroids generated from patient-derived breast cancer tissue. As a readout for cell viability of the spheroids upon drug treatment, we chose a simple size assessment from bright-field images, as well as a luminescence-based ATP assay. We show that the reduction in spheroid size correlates with a decrease in intracellular ATP levels. All tested first line chemotherapy drugs for breast cancer affected the viability of the spheroids, as expected. An optimal screening of such a drug panel would consist of dose-response data of compounds to estimate an appropriate dose for each drug regimen. Due to the relatively low yield of viable single cells extracted from breast cancer tissues, we were not able to generate enough spheroids to perform such analysis. However, in general, there are many challenges in the translation of doses determined in vitro to clinical dosing. Furthermore, the goal of a personalized medicine assay is foremost to assess the drugs and drug combinations to which an individual tumor is sensitive, rather than to provide exact dosing information

Here, our main focus was to investigate spheroids for their specificity and sensitivity towards specific drugs as single agent application which were selected based on their clinical relevance for the tumor type. This valid, biological platform can significantly contribute to the choice of first-line treatment where single or combinatorial drugs are used for a better therapeutic response in individual patients. Additionally, the time frame of spheroid cultures enables the investigation of tumor relapse in vitro, providing a valuable tool for predicting drug resistance in vivo. Shuford et al. have recently reported that spheroids generated

from ovarian tissues accurately predicted the response and non-response of ovarian cancer patients to specific treatments.

Summary: Benefits and limitations of the spheroid model

3D models provide enormous benefit beyond conventional 2D cell culture models with regards to establishing an efficient in vitro pre-clinical platform for drug screening that accurately represents the original tumor (Morgan et al., 2016; Shuford et al., 2019; Weydert et al., 2020). Several 3D models have been developed including organoids, tissue slices, hydrogels, bioreactors, microfluidic models and scaffold-free spheroids (Bolck et al., 2019; Brancato et al., 2020; Grinshpun et al., 2018; Jo et al., 2018; Majumder et al., 2015; Morgan et al., 2016; Orditura et al., 2018; Tanigawa et al., 2016; Weiswald et al., 2015). In our research, we investigated the utility of spheroids as a model for drug testing on patient-derived breast cancer tissue. The benefits and limitations of this technique are listed in Table 2. One of the primary limitations, that is true of all 3D culture methods, is the unpredictable quality of human biopsies and surgical resections as source of starting material. The tissue heterogeneity and size differ between various tissue types. Ultimately, breast tissue contains a high percentage of fat cells and a relatively low volume of epithelial cells, whereas other tissue types, such as colon or prostate yield a higher number of viable cancer cells (our unpublished data and (Goldhammer et al., 2019)). Despite the challenges presented with the starting tissue in breast cancer we were able to generate spheroids with the relatively high success rate of nearly 90%. Before this model can be firmly established as a viable system for prediction of drug efficacy a more thorough investigation of the subpopulations that exist in the original tumor and the spheroids must be performed.

Notably, the biggest advantage of our method, which utilizes the Corning® ULA microplates and the InSphero 3D InSight™ system is the straightforward seeding procedure and the ease of plate handling. In addition, within only a few days, spheroids are already visible and functional for drug treatment and respective end-point assays. Therefore, they provide a promising tool for pre-clinical prediction of drug response in personalized cancer therapy.

Overall, our success rate in generating spheroids from nearly 90% of the breast cancer tissue samples obtained, as well as the rapid time frame, use of minimal equipment, and flexibility, support the potential of this method for clinical application.

Table 2
Summary of benefits and limitations of 3D spheroid models

Advantages/ Benefits	Disadvantages/ Technical limitations
<ul style="list-style-type: none"> • easy to handle (cells are simply seeded into the wells) • suitable for high-throughput assay • scaffold-free • rapid growth (spheroids can be seen on average after 4–6 days in culture), and thus rapid response evaluation • overall success rate: >80% • recapitulation of genetic markers from the original tissue in the spheroids • many potential end-point assays (IHC, cell viability, genomics, transcriptomics, etc.) • determination of IC50 for drugs • can potentially be applied in personalized medicine 	<ul style="list-style-type: none"> • large amount of starting materials needed • tissue quality is critical (viable cells needed for viability assays) • susceptible to contamination • handling of tissue in operation room and transportation conditions are critical • undefined composition of epithelial and non-epithelial cells (fibroblasts, immune cells) • cryo-preservation of immune cells is not possible • potential selection and enrichment of certain subpopulations depending on media composition and growth conditions • determined IC50 values might not reflect clinical applicability • necessity of large number of spheroids to conduct dose-response and drug combination studies in high-throughput format

Materials And Methods:

Collection of Patient samples:

All tissue samples were collected between August 2018 until December 2019. Breast cancer samples were received from the Institutional Biobank at Tel Aviv Sourasky Medical Center in accordance with the Helsinki committee-approved protocol (No. 0282-18-TLV) and under the relevant ethical guidelines and regulations. Informed consent was obtained from all patients.

The samples were received by the biobank directly after surgery and were transported to our laboratory on ice in sterile tubes containing HypoThermosol® FRS medium (StemCell Technologies). Tissue was processed within 72 hours of surgery. Sample and clinical information about the patient were acquired anonymously, with identifying information encoded at the clinical site.

Generation of spheroids:

The tissue was placed in a sterile 10 cm dish, photographed, and cut into 1–3 mm³ pieces using a sterile razor blade. Representative pieces were saved for IHC analysis of the original tissue. The rest was further minced. Eventually, all remaining tissue was placed in a falcon tube containing Advanced DMEM

supplemented with 1% Glutamax, 1% HEPES 1M, 1% Pen/Strep (all Gibco), 1x primocin (InvivoGen), 0.5 mg/ml collagenase (Sigma) and 0.2 mg/ml DNase I (Sigma), and incubated on an orbital shaker at 220 rpm, at 37 °C for up to 16 hrs. Where necessary, an additional digestion with 1x TrypLE (Gibco) was performed for 10 min at 37 °C. Then, red blood cells were eliminated using the BD Pharm Lyse™ Lysing Buffer (BD Biosciences) according to the manufacturer's instructions. Finally, the cell suspension was strained over 40 um Corning® cell strainers (Corning), and the single cell yield was assessed using the LUNA™ cell counter. Spheroids were generated using either the 3D InSight™ (GravityTRAP™ and GravityPLUS™) Hanging Drop System (InSphero AG) or the Corning® ULA spheroid microplates (Corning CLS4515) according to the manufacturer's instructions. 1000 patient-derived cells were seeded in co-culture with HDFs (Sigma 106-05A) in a ratio of 1:1 or 1:3 per well in a 96-well plate format. Spheroids were grown in Mammary Epithelial Basal Medium (Lonza) supplemented with 2 mM L-Glutamine, 1% Penicillin-Streptomycin, 1% Fetal Bovine Serum (all Gibco), 5 ug/ml insulin (PromoCell), 0.5 ug/ml Hydrocortisone, 20 ng/ml EGF, 20 ng/ml human FGF10, 1 U/ml Heparin, 50 uM L-Ascorbic acid, 50 ng/ml Cholera Toxin, 35 ug/ml BPE (all Sigma), 1x B27 supplement (Life Technologies) and 20 ng/ml beta-Estradiol (Sigma). Media was changed every 2–3 days and spheroid growth was monitored by light microscopy using the Zeiss Axio Observer fluorescent microscope.

Histology and IHC:

Spheroids and original tissue pieces were collected into 1.5 ml Eppendorf tubes, washed in 1x PBS and fixed with 4% Paraformaldehyde (Bar Naor Ltd) for 15 min at RT. All further histology and IHC steps were performed by the staff of PathoLab (Rehovot, Israel). H&E staining was done using the Tissue Tek Prisma device under standard conditions. IHC staining for specific markers was done using the Ventana BenchMark Ultra System, and the following antibodies were used at the following dilutions:

Table 3
Antibodies used in this study for IHC

Marker	Antibody	Catalogue number	Dilution
ER	Rabbit monoclonal anti-Human ER, clone SP1	Ventana cat# 790-4325	RTU
PR	Mouse monoclonal anti-Human PRA, clone 16	Leica Cat# NCL-L-PGR-312	1:100
Her2	Rabbit monoclonal anti-Human Her2/new, clone 4B5	Ventana cat# 790-2991	RTU
CK	Mouse monoclonal anti-Human cytokeratin, clone AE1/AE3	Dako cat#M3515	1:200
Gata3	Mouse monoclonal anti-Human Gata3, clone L50-823	Zytomed, cat#BMS054	RTU
Vimentin	Mouse monoclonal anti-Human Vimentin, clone V9	Dako, cat#M0725	1:1000
Mammaglobin	Mouse monoclonal anti-Human Mammaglobin, clone 304-1A5	Dako, cat#IS074	RTU

Drug panel and CellTiter-Glo® 3D Cell Viability Assay:

Breast cancer patient-derived spheroids were cultured in InSphero 3D InSight™ plates for 4 days. The following compounds were applied in 5 replicates per treatment at the respective final concentration: 2 µM Doxo (D1515), 100 nM Pac (T7191), 50 µg/ml 5-FU (F6627), 1 µM Epi (E9406), 20 mM Met (PHR1084, all Sigma Aldrich). Redosing was performed after 3 days, and viability of the spheroids was determined after 7 days of treatment with the CellTiter-Glo® 3D Cell Viability Assay (Promega G9682) according to the manufacturer's instructions. Luminescence readout was read in CLARIOstar® Plus plate reader (BMG LABTECH). The mean of absolute luminescence from 5 replicates and the standard error was determined. Graphs were generated using GraphPad Prism. Student's t-test and two-way ANOVA were performed for statistical analysis.

Abbreviations

5-Fluorouracil	5-FU
Chemotherapy sensitivity and resistance assays	CSRAs
Doxorubicin	Doxo
Epirubicin	Epi
Human dermal fibroblasts	HDF
Immunofluorescence	IF
Immunohistochemistry	IHC
Metformin	Met
Paclitaxel	Pac
Pan Cytokeratin	panCK
Three dimensional	3D
Two dimensional	2D
Ultra-Low Attachment	ULA

Declarations

Ethics approval and consent to participate

All tissue samples were received from the Institutional Biobank at Tel Aviv Sourasky Medical Center in accordance with the Helsinki committee-approved protocol (No. 0282-18-TLV) and under the relevant ethical guidelines and regulations. Informed consent was obtained from all patients.

Consent for publication

Not applicable.

Availability of data and materials

All clinical data from all patient-derived samples are included in this published article as supplementary table 1.

Competing interests

The authors declare that they have no competing interests.

Funding

This study was funded by internal funds of the Institute of Personalized and Translational Medicine at Ariel University, Israel. The funding body was not involved in the design of the study, nor in data collection, analysis, and interpretation of data, nor in the writing of the manuscript.

Authors' contributions

SH, RCH and IK designed the research. SH performed the experiments. SH and YM analyzed and interpreted the data. SH, RCH and YM wrote the manuscript. IK acquired funding and gave intellectual input. All authors read and approved the final manuscript.

Acknowledgement

We thank Olga Shovman, Nili Turian, Karin Abeav, Hadas Fulman-Levy, and Tzachi Morad for technical assistance, and Dr. Sharona Even Ram for comments on the manuscript (all from the Institute for Personalized and Translational Medicine). We are grateful to Drs. Francesca Chiovaro, Wolfgang Moritz (both InSphero AG, Switzerland) and Sumeer Dhar for helpful discussions and comments on the study and the manuscript. We also thank Dr. Ayelet Izhaki and coworkers from the Institutional Biobank at Tel Aviv Sourasky Medical Center for help in collecting surgical specimens.

References

1. Amann A, Zwierzina M, Gamerith G, Bitsche M, Huber JM, Vogel GF, Blumer M, Koeck S, Pechriggl EJ, Kelm JM, et al. Development of an innovative 3D cell culture system to study tumour–stroma interactions in non-small cell lung cancer cells. *PLoS ONE*. 2014;9:e92511.
2. Anastasov N, Höfig I, Radulović V, Ströbel S, Salomon M, Lichtenberg J, Rothenaigner I, Hadian K, Kelm JM, Thirion C, et al. A 3D-microtissue-based phenotypic screening of radiation resistant tumor cells with synchronized chemotherapeutic treatment. *BMC Cancer*. 2015;15:466.
3. Bastien JIL, McNeill KA, Fine HA. Molecular characterizations of glioblastoma, targeted therapy, and clinical results to date. *Cancer*. 2015;121:502–16.
4. Bolck HA, Corrà C, Kahraman A, von Teichman A, Toussaint NC, Kuipers J, Chiovaro F, Koelzer VH, Pauli C, Moritz W, et al. (2019). Tracing Clonal Dynamics Reveals that Two- and Three-dimensional Patient-derived Cell Models Capture Tumor Heterogeneity of Clear Cell Renal Cell Carcinoma. *Eur Urol Focus*.
5. Brancato V, Oliveira JM, Correlo VM, Reis RL, Kundu SC. (2020). Could 3D models of cancer enhance drug screening? *Biomaterials* 232, 119744.
6. Burstein HJ, Mangu PB, Somerfield MR, Schrag D, Samson D, Holt L, Zelman D, Ajani JA. American Society of Clinical Oncology. (2011). American Society of Clinical Oncology clinical practice

- guideline update on the use of chemotherapy sensitivity and resistance assays. *J Clin Oncol* 29, 3328–30.
7. Buxant F, Kindt N, Noël J-C, Laurent G, Saussez S. Preexposure of MCF-7 breast cancer cell line to dexamethasone alters the cytotoxic effect of paclitaxel but not 5-fluorouracil or epirubicin chemotherapy. *Breast Cancer*. 2017;9:171–5.
 8. Cardoso F, Kyriakides S, Ohno S, Penault-Llorca F, Poortmans P, Rubio IT, Zackrisson S, Senkus E. (2019). Early breast cancer: ESMO Clinical Practice Guidelines for diagnosis, treatment and follow-up. *Ann. Oncol*.
 9. Coates AS, Winer EP, Goldhirsch A, Gelber RD, Gnant M, Piccart-Gebhart M, Thürlimann B, Senn H-J, Members P. Tailoring therapies—improving the management of early breast cancer: St Gallen International Expert Consensus on the Primary Therapy of Early Breast Cancer 2015. *Ann Oncol*. 2015;26:1533–46.
 10. Coyle C, Cafferty FH, Vale C, Langley RE. Metformin as an adjuvant treatment for cancer: a systematic review and meta-analysis. *Ann Oncol*. 2016;27:2184–95.
 11. Denkert C, Liedtke C, Tutt A, von Minckwitz G. Molecular alterations in triple-negative breast cancer—the road to new treatment strategies. *Lancet*. 2017;389:2430–42.
 12. Duffy MJ, Harbeck N, Nap M, Molina R, Nicolini A, Senkus E, Cardoso F. Clinical use of biomarkers in breast cancer: Updated guidelines from the European Group on Tumor Markers (EGTM). *Eur J Cancer*. 2017;75:284–98.
 13. Falkenberg N, Anastasov N, Höfig I, Bashkueva K, Lindner K, Höfler H, Rosemann M, Aubele M. Additive impact of HER2-/PTK6-RNAi on interactions with HER3 or IGF-1R leads to reduced breast cancer progression in vivo. *Mol Oncol*. 2015;9:282–94.
 14. Falkenberg N, Höfig I, Rosemann M, Szumielewski J, Richter S, Schorpp K, Hadian K, Aubele M, Atkinson MJ, Anastasov N. Three-dimensional microtissues essentially contribute to preclinical validations of therapeutic targets in breast cancer. *Cancer Med*. 2016;5:703–10.
 15. Fotheringham S, Mozolowski GA, Murray EMA, Kerr DJ. Challenges and solutions in patient treatment strategies for stage II colon cancer. *Gastroenterol Rep (Oxf)*. 2019;7:151–61.
 16. Garbar C, Mascaux C, Giustiniani J, Merrouche Y, Bensussan A. Chemotherapy treatment induces an increase of autophagy in the luminal breast cancer cell MCF7, but not in the triple-negative MDA-MB231. *Sci Rep*. 2017;7:7201.
 17. Goldhammer N, Kim J, Timmermans-Wielenga V, Petersen OW. Characterization of organoid cultured human breast cancer. *Breast Cancer Res*. 2019;21:141.
 18. Goldman A, Majumder B, Dhawan A, Ravi S, Goldman D, Kohandel M, Majumder PK, Sengupta S. Temporally sequenced anticancer drugs overcome adaptive resistance by targeting a vulnerable chemotherapy-induced phenotypic transition. *Nat Commun*. 2015;6:6139.
 19. Griguolo G, Dieci MV, Guarneri V, Conte P. Olaparib for the treatment of breast cancer. *Expert Rev Anticancer Ther*. 2018;18:519–30.

20. Grinshpun A, Gavert N, Granit RZ, Masuri H, Ben-Porath I, Breuer S, Zick A, Rosenberg S, Maoz M, Granit A, et al. Ev vivo organ culture as potential prioritization tool for breast cancer targeted therapy. *Cancer Biol Ther.* 2018;19:645–8.
21. Gu G, Dustin D, Fuqua SA. Targeted therapy for breast cancer and molecular mechanisms of resistance to treatment. *Curr Opin Pharmacol.* 2016;31:97–103.
22. Halfter K, Hoffmann O, Ditsch N, Ahne M, Arnold F, Paepke S, Grab D, Bauerfeind I, Mayer B. Testing chemotherapy efficacy in HER2 negative breast cancer using patient-derived spheroids. *J Transl Med.* 2016;14:112.
23. Heimes A-S, Schmidt M. Atezolizumab for the treatment of triple-negative breast cancer. *Expert Opin Investig Drugs.* 2019;28:1–5.
24. Herter S, Morra L, Schlenker R, Sulcova J, Fahrni L, Waldhauer I, Lehmann S, Reisländer T, Agarkova I, Kelm JM, et al. A novel three-dimensional heterotypic spheroid model for the assessment of the activity of cancer immunotherapy agents. *Cancer Immunol Immunother.* 2017;66:129–40.
25. Hickman JA, Graeser R, de Hoogt R, Vidic S, Brito C, Gutekunst M, van der Kuip H. IMI PREDECT Consortium. (2014). Three-dimensional models of cancer for pharmacology and cancer cell biology: capturing tumor complexity in vitro/ex vivo. *Biotechnol J* 9, 1115–28.
26. Ho WY, Yeap SK, Ho CL, Rahim RA, Alitheen NB. (2012). Development of Multicellular Tumor Spheroid (MCTS) Culture from Breast Cancer Cell and a High Throughput Screening Method Using the MTT Assay. *PLoS One* 7.
27. Hollenberg MD, Cuatrecasas P. (1973). Epidermal growth factor: receptors in human fibroblasts and modulation of action by cholera toxin. *Proc. Natl. Acad. Sci. U.S.A.* 70, 2964–2968.
28. Howlader N, Cronin KA, Kurian AW, Andridge R. Differences in Breast Cancer Survival by Molecular Subtypes in the United States. *Cancer Epidemiol Biomarkers Prev.* 2018;27:619–26.
29. Huang T-C, Campbell TC. Comparison of weekly versus every 3 weeks paclitaxel in the treatment of advanced solid tumors: a meta-analysis. *Cancer Treat Rev.* 2012;38:613–7.
30. Hultsch S, Kankainen M, Paavolainen L, Kovanen R-M, Ikonen E, Kangaspeska S, Pietiäinen V, Kallioniemi O. Association of tamoxifen resistance and lipid reprogramming in breast cancer. *BMC Cancer.* 2018;18:850.
31. I C, S, G., and Al H. (2010). Efficacy of Anti-Cancer Agents in Cell Lines Versus Human Primary Tumour Tissue.
32. Jamdade VS, Sethi N, Mundhe NA, Kumar P, Lahkar M, Sinha N. Therapeutic targets of triple-negative breast cancer: a review. *Br J Pharmacol.* 2015;172:4228–37.
33. Jensen BV. Cardiotoxic consequences of anthracycline-containing therapy in patients with breast cancer. *Semin Oncol.* 2006;33:15–21.
34. Jo Y, Choi N, Kim K, Koo H-J, Choi J, Kim HN. (2018). Chemoresistance of Cancer Cells: Requirements of Tumor Microenvironment-mimicking In Vitro Models in Anti-Cancer Drug Development. *Theranostics* 8, 5259–5275.

35. Joo WD, Lee JY, Kim JH, Yoo HJ, Roh HJ, Park JY, Kim DY, Kim YM, Kim YT, Nam JH. Efficacy of taxane and platinum-based chemotherapy guided by extreme drug resistance assay in patients with epithelial ovarian cancer. *J Gynecol Oncol.* 2009;20:96–100.
36. Kijima T, Nakagawa H, Shimonosono M, Chandramouleeswaran PM, Hara T, Sahu V, Kasagi Y, Kikuchi O, Tanaka K, Giroux V, et al. Three-Dimensional Organoids Reveal Therapy Resistance of Esophageal and Oropharyngeal Squamous Cell Carcinoma Cells. *Cell Mol Gastroenterol Hepatol.* 2019;7:73–91.
37. Lee GY, Kenny PA, Lee EH, Bissell MJ. Three-dimensional culture models of normal and malignant breast epithelial cells. *Nat Methods.* 2007;4:359–65.
38. Majumder B, Baraneedharan U, Thiyagarajan S, Radhakrishnan P, Narasimhan H, Dhandapani M, Brijwani N, Pinto DD, Prasath A, Shanthappa BU, et al. Predicting clinical response to anticancer drugs using an ex vivo platform that captures tumour heterogeneity. *Nat Commun.* 2015;6:6169.
39. de Melo Gagliato D, Jardim DLF, Marchesi MSP, Hortobagyi GN. Mechanisms of resistance and sensitivity to anti-HER2 therapies in HER2 + breast cancer. *Oncotarget.* 2016;7:64431–46.
40. Memarzadeh S, Xin L, Mulholland DJ, Mansukhani A, Wu H, Teitell MA, Witte ON. Enhanced paracrine FGF10 expression promotes formation of multifocal prostate adenocarcinoma and an increase in epithelial androgen receptor. *Cancer Cell.* 2007;12:572–85.
41. Miyoshi H, Maekawa H, Kakizaki F, Yamaura T, Kawada K, Sakai Y, Taketo MM. An improved method for culturing patient-derived colorectal cancer spheroids. *Oncotarget.* 2018;9:21950–64.
42. Morgan MM, Johnson BP, Livingston MK, Schuler LA, Alarid ET, Sung KE, Beebe DJ. Personalized in vitro Cancer Models to Predict Therapeutic Response: Challenges and a Framework for Improvement. *Pharmacol Ther.* 2016;165:79–92.
43. Mulholland T, McAllister M, Patek S, Flint D, Underwood M, Sim A, Edwards J, Zagnoni M. Drug screening of biopsy-derived spheroids using a self-generated microfluidic concentration gradient. *Sci Rep.* 2018;8:14672.
44. Neumayer HH, Paradis K, Korn A, Jean C, Fritsche L, Budde K, Winkler M, Kliem V, Pichlmayr R, Hauser IA, et al. Entry-into-human study with the novel immunosuppressant SDZ RAD in stable renal transplant recipients. *Br J Clin Pharmacol.* 1999;48:694–703.
45. Ni Y-B, Tsang JYS, Shao M-M, Chan S-K, Cheung S-Y, Tong J, To K-F, Tse GM. GATA-3 is superior to GCDFP-15 and mammaglobin to identify primary and metastatic breast cancer. *Breast Cancer Res Treat.* 2018;169:25–32.
46. Ochs RL, Burholt D, Kornblith P. The ChemoFx assay: an ex vivo cell culture assay for predicting anticancer drug responses. *Methods Mol Med.* 2005;110:155–72.
47. Orditura M, Della Corte CM, Diana A, Ciaramella V, Franzese E, Famiglietti V, Panarese I, Franco R, Grimaldi A, Lombardi A, et al. Three dimensional primary cultures for selecting human breast cancers that are sensitive to the anti-tumor activity of ipatasertib or taselisib in combination with anti-microtubule cytotoxic drugs. *Breast.* 2018;41:165–71.

48. O'Shaughnessy J, Beck T, J., and Royce M. Everolimus-based combination therapies for HR+, HER2-metastatic breast cancer. *Cancer Treat Rev.* 2018;69:204–14.
49. Poudel P, Nyamundanda G, Patil Y, Cheang MCU, Sadanandam A. Heterocellular gene signatures reveal luminal-A breast cancer heterogeneity and differential therapeutic responses. *NPJ Breast Cancer.* 2019;5:21.
50. Richard S, Wells A, Connor J, Price F. (2015). Use of ChemoFx® for Identification of Effective Treatments in Epithelial Ovarian Cancer. *PLoS Curr* 7.
51. Rimann M, Latenser S, Gvozdenovic A, Muff R, Fuchs B, Kelm JM, Graf-Hausner U. An in vitro osteosarcoma 3D microtissue model for drug development. *J Biotechnol.* 2014;189:129–35.
52. Shuford S, Wilhelm C, Rayner M, Elrod A, Millard M, Mattingly C, Lotstein A, Smith AM, Guo QJ, O'Donnell L, et al. Prospective Validation of an Ex Vivo, Patient-Derived 3D Spheroid Model for Response Predictions in Newly Diagnosed Ovarian Cancer. *Sci Rep.* 2019;9:11153.
53. Tanigawa N, Yamaue H, Ohyama S, Sakuramoto S, Inada T, Kodera Y, Kitagawa Y, Omura K, Terashima M, Sakata Y, et al. Exploratory phase II trial in a multicenter setting to evaluate the clinical value of a chemosensitivity test in patients with gastric cancer (JACCRO-GC 04, Kubota memorial trial). *Gastric Cancer.* 2016;19:350–60.
54. Telli ML, Gradishar WJ, Ward JH. NCCN Guidelines Updates: Breast Cancer. *J Natl Compr Canc Netw.* 2019;17:552–5.
55. Thoma CR, Stroebel S, Rösch N, Calpe B, Krek W, Kelm JM. A high-throughput-compatible 3D microtissue co-culture system for phenotypic RNAi screening applications. *J Biomol Screen.* 2013;18:1330–7.
56. Thoma CR, Zimmermann M, Agarkova I, Kelm JM, Krek W. 3D cell culture systems modeling tumor growth determinants in cancer target discovery. *Adv Drug Deliv Rev.* 2014;69–70:29–41.
57. Walsh V, Goodman J. From taxol to Taxol: the changing identities and ownership of an anti-cancer drug. *Med Anthropol.* 2002;21:307–36.
58. Weiswald L-B, Bellet D, Dangles-Marie V. Spherical Cancer Models in Tumor Biology Neoplasia. 2015;17:1–15.
59. Weydert Z, Lal-Nag M, Mathews-Greiner L, Thiel C, Cordes H, Küpfer L, Guye P, Kelm JM, Ferrer M. A 3D Heterotypic Multicellular Tumor Spheroid Assay Platform to Discriminate Drug Effects on Stroma versus Cancer Cells. *SLAS Discov.* 2020;25:265–76.
60. Whelan KA, Muir AB, Nakagawa H. Esophageal 3D Culture Systems as Modeling Tools in Esophageal Epithelial Pathobiology and Personalized Medicine. *Cell Mol Gastroenterol Hepatol.* 2018;5:461–78.
61. Yin X, Mead BE, Safaee H, Langer R, Karp JM, Levy O. Engineering Stem Cell Organoids. *Cell Stem Cell.* 2016;18:25–38.
62. Yuan C, Liu Z, Yu Q, Wang X, Bian M, Yu Z, Yu J. Expression of PD-1/PD-L1 in primary breast tumours and metastatic axillary lymph nodes and its correlation with clinicopathological parameters. *Sci Rep.* 2019;9:14356.

63. Zasadil LM, Andersen KA, Yeum D, Rocque GB, Wilke LG, Tevaarwerk AJ, Raines RT, Burkard ME, Weaver BA. Cytotoxicity of paclitaxel in breast cancer is due to chromosome missegregation on multipolar spindles. *Sci Transl Med.* 2014;6:229ra43.
64. Zoli W, Ulivi P, Tesi A, Fabbri F, Rosetti M, Maltoni R, Giunchi DC, Ricotti L, Briigliadori G, Vannini I, et al. Addition of 5-fluorouracil to doxorubicin-paclitaxel sequence increases caspase-dependent apoptosis in breast cancer cell lines. *Breast Cancer Res.* 2005;7:R681–9.

Figures

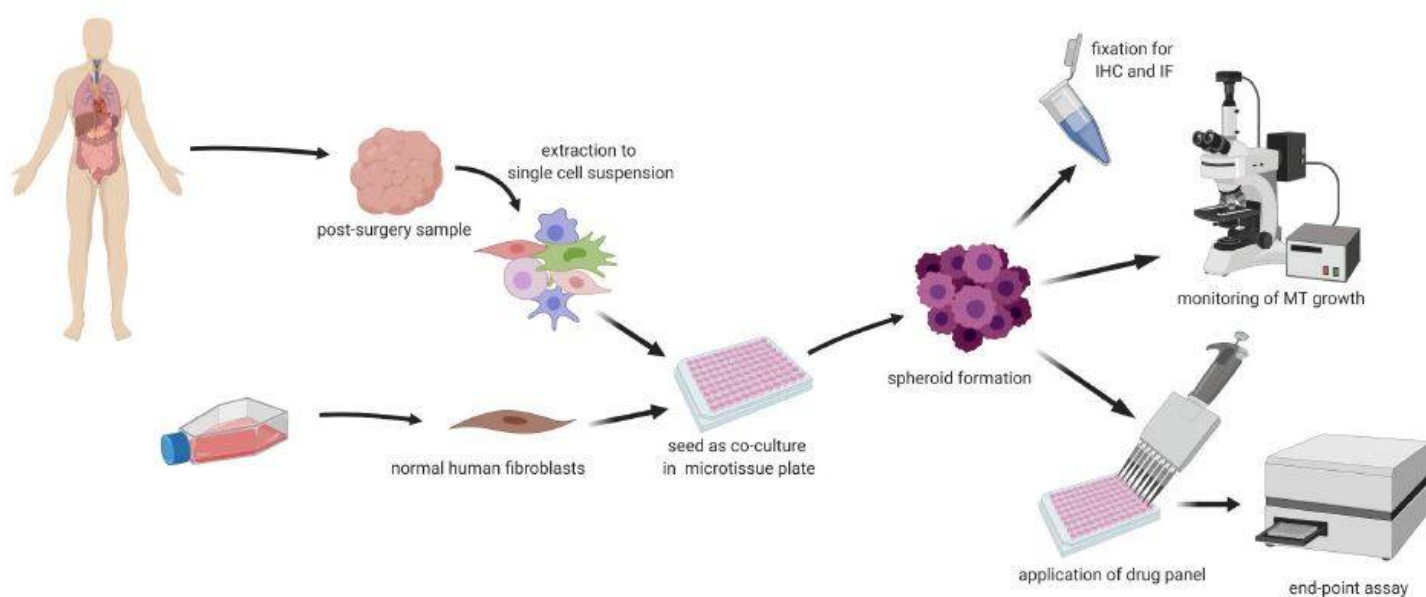


Figure 1

Workflow Surgical resections of previously untreated tumors were dissociated into a single cell solution and seeded together with cultured normal human fibroblasts in specialized plates. Spheroids were maintained, monitored over time, and analyzed by a variety of end-point assays including ATP production, cell viability, and IHC assays. (made in ©BioRender - biorender.com)

Tumor:Fibroblast ratios

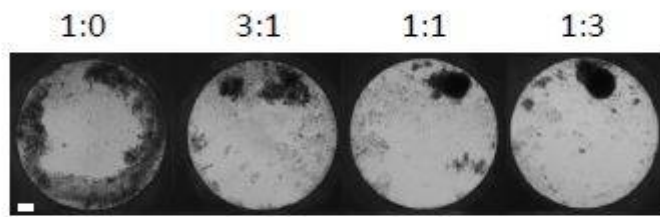


Figure 2

A ratio of 1:3 is the optimal ratio of tumor cells to fibroblasts for spheroid growth. Tumor cells were seeded with varying ratios of normal human fibroblast. Spheroids were grown for 7 days under optimal growth conditions. Spheroids grown from this proportion exhibit a tightly packed, round, and spherical form. Scale bar = 100 μ m

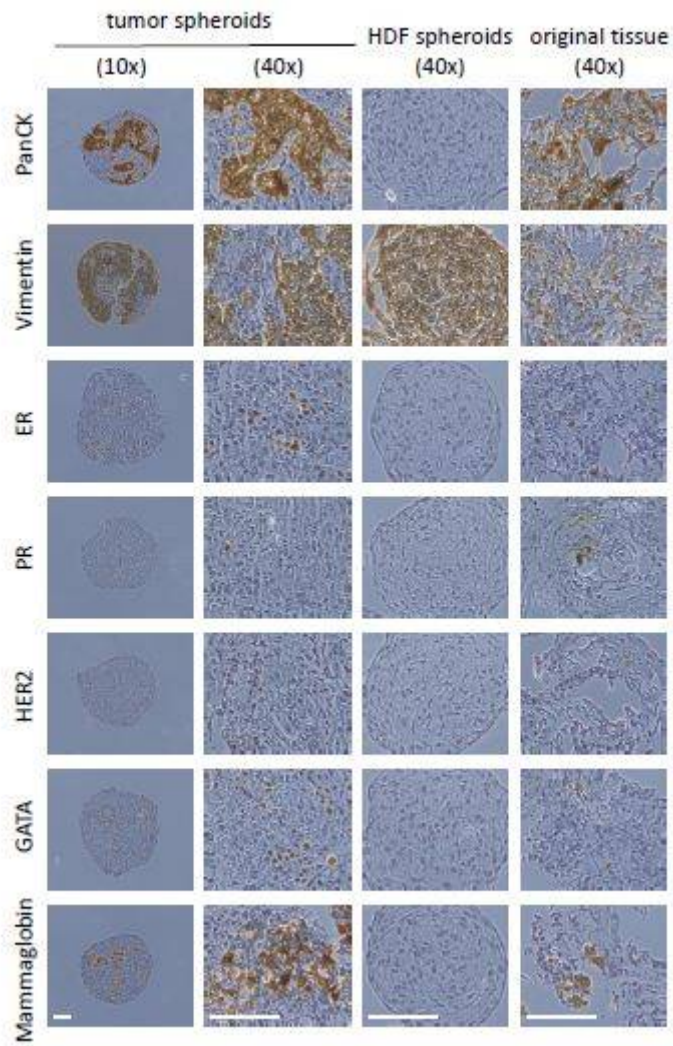


Figure 3

IHC staining of breast cancer spheroids reveals the heterogenous mixture of cellular components within the spheroids: epithelial marker (PanCK), fibroblast marker (Vimentin), ER, PR, Her2, Mammaglobin, GATA. The IHC staining of the spheroids resembles that of the original tissue (ER+, PR-, Her2-, luminal B i). Scale bar = 100 μ m

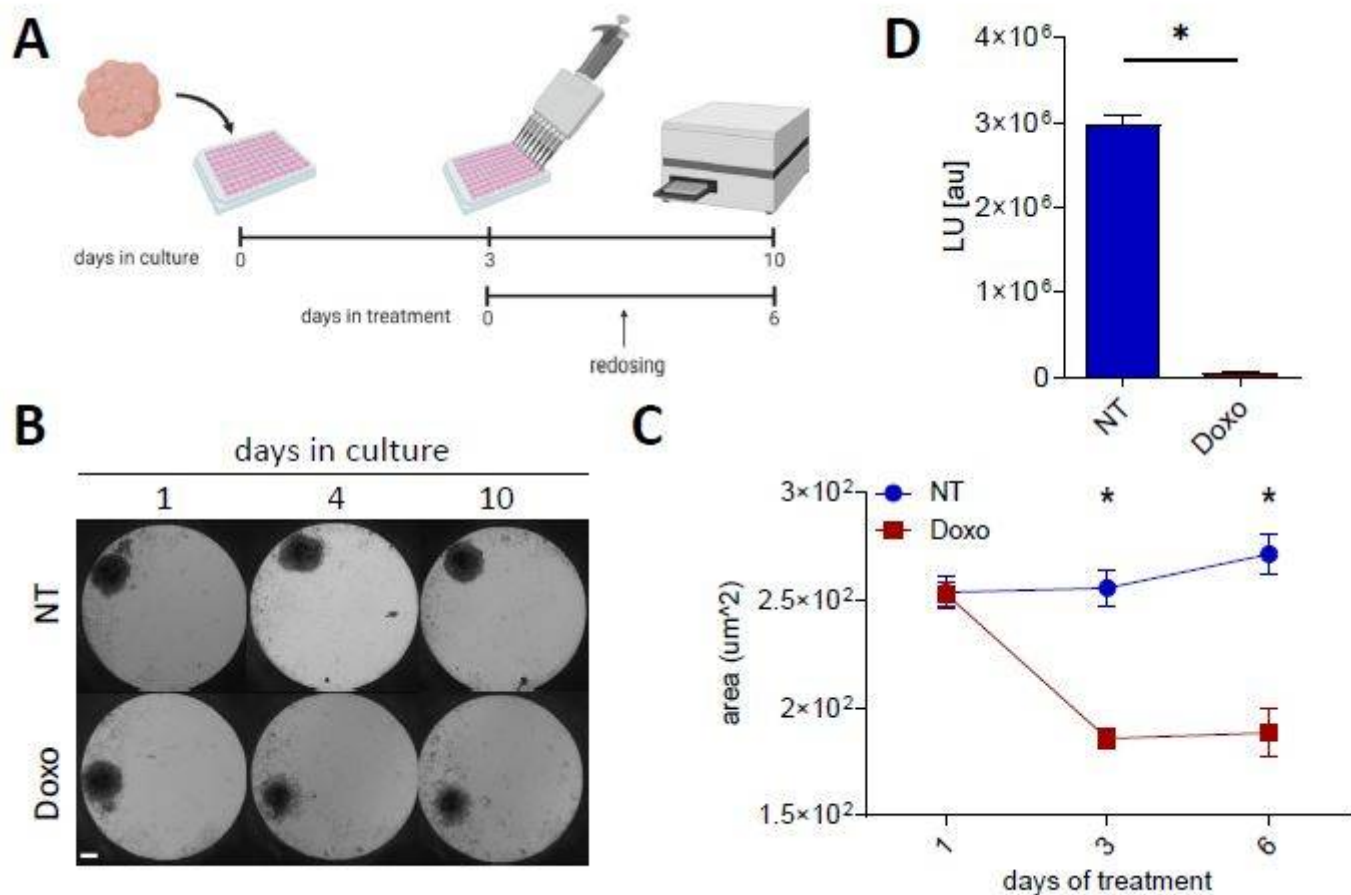


Figure 4

Spheroids respond to treatment with Doxorubicin. (A) Schematic representation of the experimental framework and timeline (made in ©BioRender - biorender.com). (B) Phase contrast images of spheroids built from breast cancer tissue (ER+, PR-, Her2-, luminal B i) in InSphero3D InSight™ plates. Spheroids were treated with 2 μM Doxo after 4 days in culture. Redosing was done on day 3. Spheroid growth was monitored over 6 days of treatment and a clear shrinking of the tumor was observed (C) Growth of breast tissue spheroids was monitored throughout the 6 days of treatment (n=4, asterisks indicate statistically significant differences from the NT; p<0.004, analyzed using two-way ANOVA, followed by Bonferroni's test). (D) ATP levels of breast tissue spheroids following 7 days of Doxo treatment was assessed using a luminescence-based ATP assay. A significant decrease in intracellular ATP levels was observed in Doxo-treated spheroids, which correlated with the reduction in tumor volume (n=4, asterisks indicate statistically significant differences from the NT; p<0.001, analyzed using two-tailed, unpaired Student's t-test. Scale bar = 100 μm

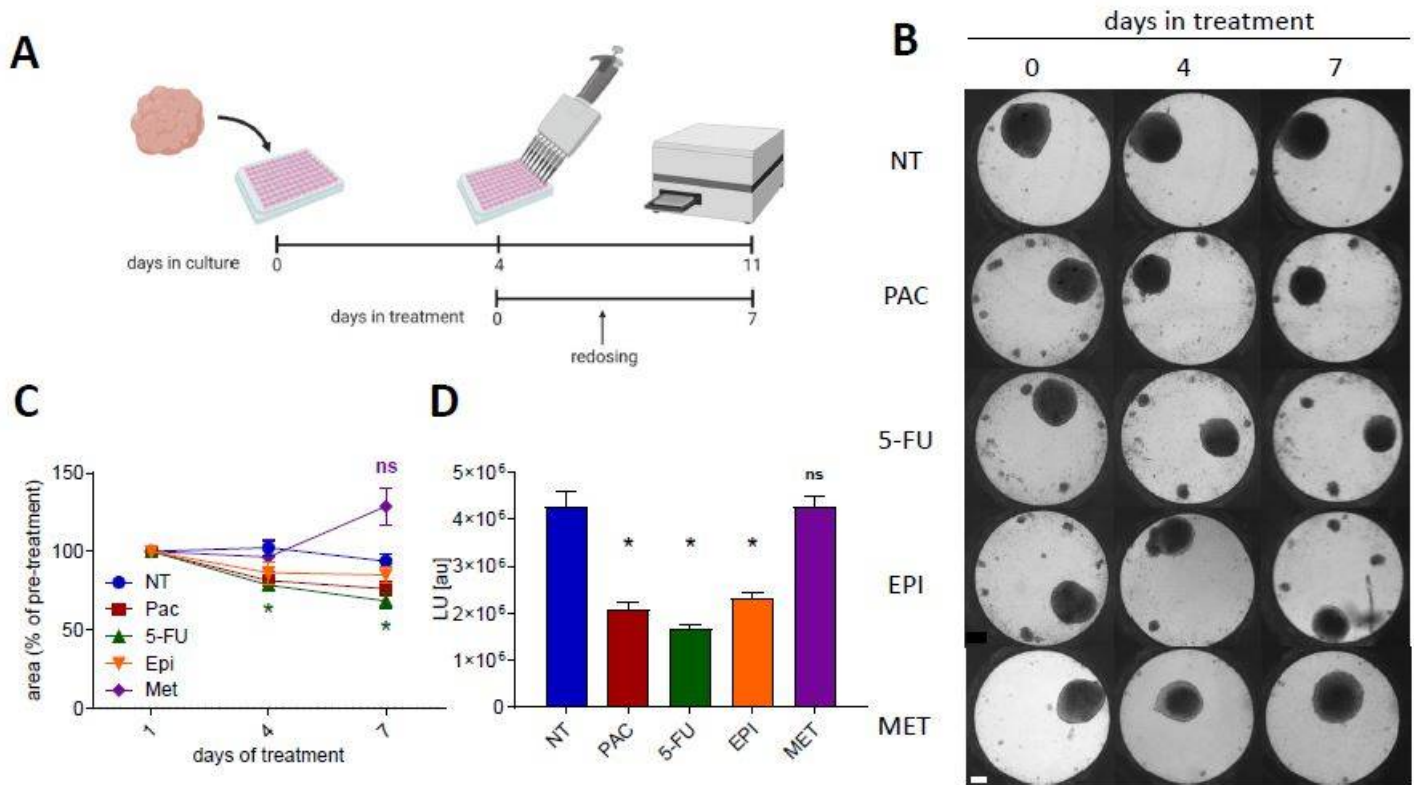


Figure 5

Drug panel reveals differences in response of breast cancer spheroids to multiple chemotherapeutic agents (A) Schematic representation of experimental framework and timeline (made in ©BioRender - biorender.com). (B) Phase contrast images track morphological changes of spheroids generated from human breast cancer samples (ER+, PR+, Her2-, luminal A) upon a 7 day treatment in InSphero 3D InSight™ plates. Drug treatment included 100 nM Pac, 50 µg/ml 5-FU, 1 µM Epi or 20 mM Met and was applied 4 days after cell seeding, in 5 replicates per treatment. Redosing was performed after 3 days. (C) Size of tumor spheroids significantly decreases in response to 5-FU treatment. Data is presented as a percent of size on day 1 of treatment (n=5, asterisks indicate statistically significant differences from the NT; p<0.05, analyzed using two-way ANOVA, followed by Dunnett's test). (D) Viability of the spheroids was determined after 7 days of treatment using a luminescence-based ATP assay. The average of absolute luminescence from 5 replicates is shown in the graph, and standard deviation is depicted. ATP levels significantly decreased under treatment with the first-line chemotherapy drugs for breast cancer, Pac, 5-FU and Epi, while Met showed no reduction in ATP levels (n=5, asterisks indicate statistically significant differences from the NT; p<0.0001, analyzed using two-way ANOVA, followed by Dunnett's test). Scale bar = 100 µm

Supplementary Files

This is a list of supplementary files associated with this preprint. Click to download.

- [Additionalfile1.docx](#)